

Supplemental Information for “Initiation of secondary nucleation in clouds”

Sylvia C. Sullivan¹, Corinna Hoose², Alexei Kiselev², Thomas Leisner², and Athanasios Nenes^{1,3,4,5}

¹School of Chemical and Biomolecular Engineering, Georgia Institute of Technology, Atlanta, GA 30332, USA

²Institute of Meteorology and Climate Research, Karlsruhe Institute of Technology, Karlsruhe, Germany

³School of Earth and Atmospheric Sciences, Georgia Institute of Technology, Atlanta, GA 30332, USA

⁴ICE-HT, Foundation for Research and Technology, Hellas, 26504 Patras, Greece

⁵IERSD, National Observatory of Athens, P. Penteli, 15236, Athens, Greece

Correspondence to: A. Nenes (athanasios.nenes@gatech.edu)

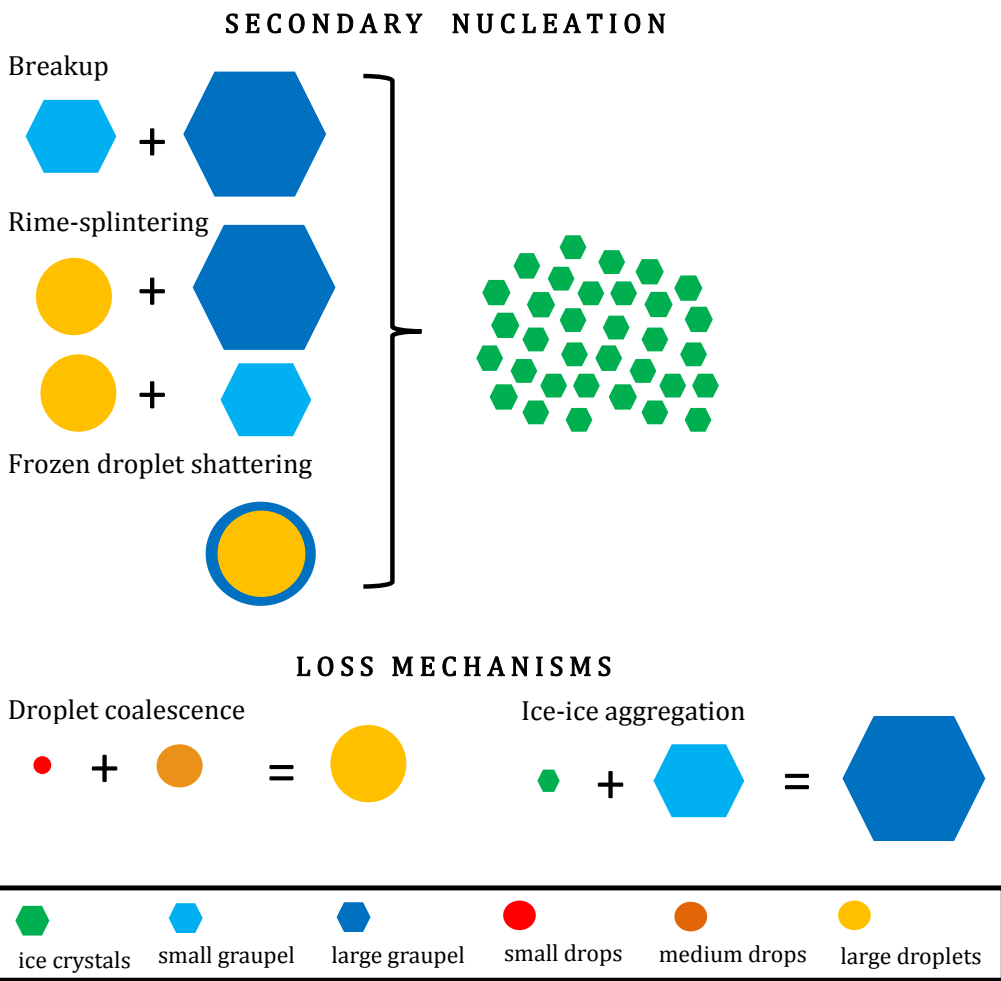


Figure S1. Schematic of the simplified six-bin microphysics model. The secondary nucleation processes included are the breakup of small and large graupel upon collision; the rime-splintering of either small or large graupel; or the shattering of large droplets upon freezing. Loss of hydrometeor number occurs through coalescence of small and medium droplets and aggregation of ice crystals and small graupel.

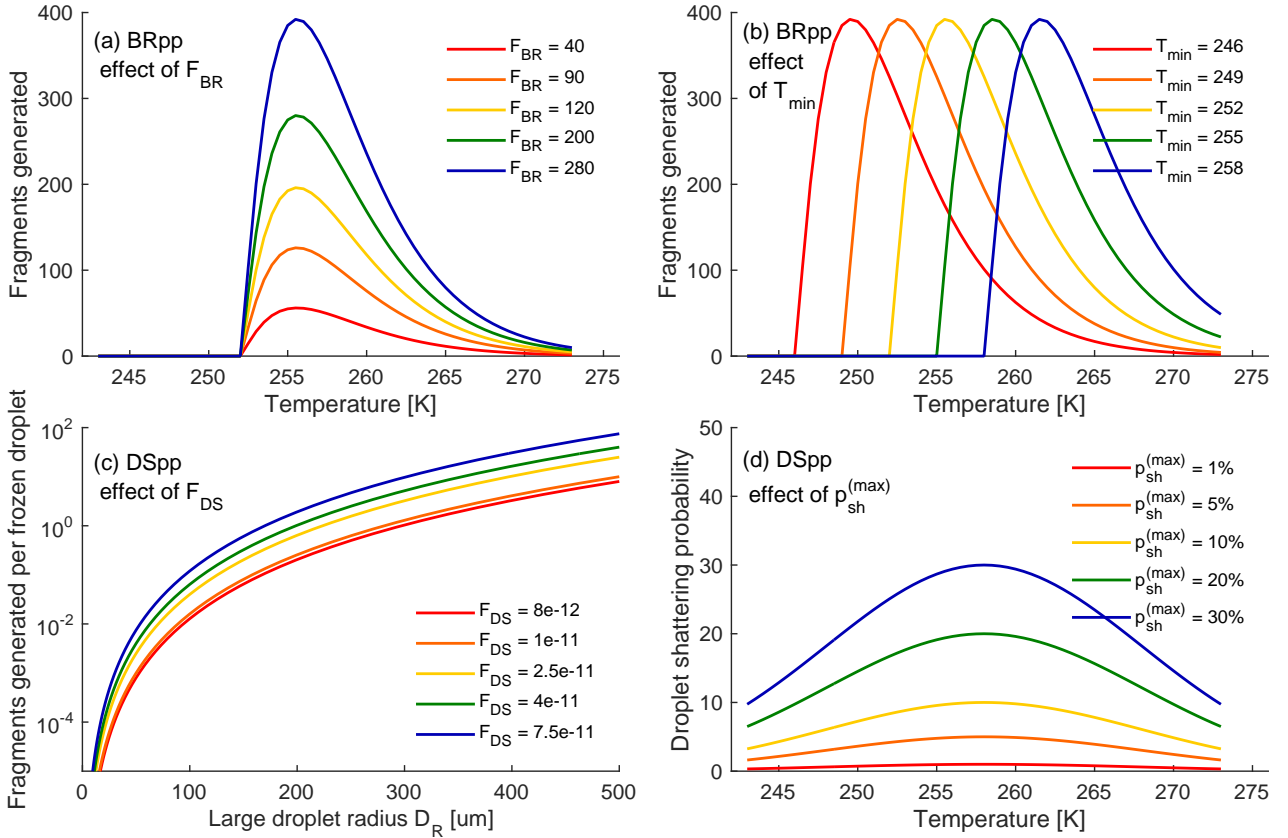


Figure S2. Effect of adjustments during the parameter perturbation simulations. Panel **(a)** shows the effect of the leading coefficient F_{BR} , and panel **(b)** the minimum temperature of occurrence, within the breakup fragmentation generation function. Panel **(c)** shows the effect of the fragments generated by shattering per frozen droplet F_{DS} , while panel **(d)** shows various temperature-dependent freezing probability distributions. Parameter values increase from red to blue.

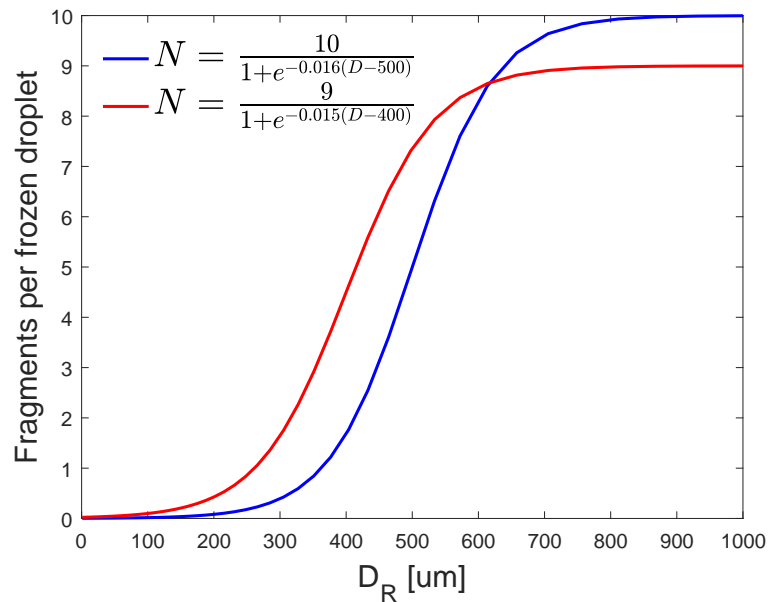


Figure S3. Alternate sigmoidal functions for the fragments generated per frozen droplet. $N_{DS}^{(sig)}$ in Table S1 below.

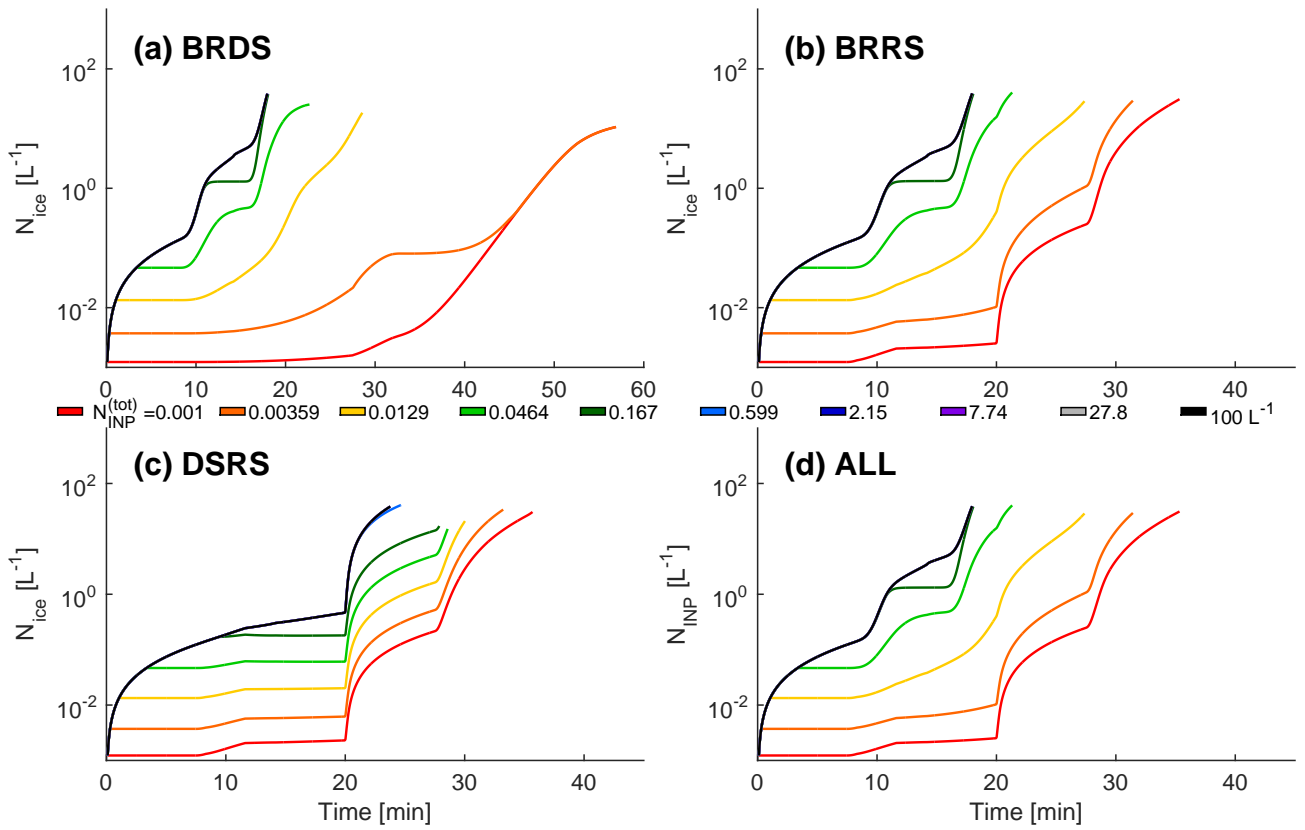


Figure S4. Evolution of the total ice hydrometeor (summation of ice crystal, small and large graupel numbers) number for default simulations with a range of $N_{INP}^{(tot)}$ from $0.001 L^{-1}$ up to $100 L^{-1}$: **(a)** breakup upon collision and droplet shattering, **(b)** breakup upon collision and rime splintering, **(c)** droplet shattering and rime splintering, and **(d)** all three processes active.

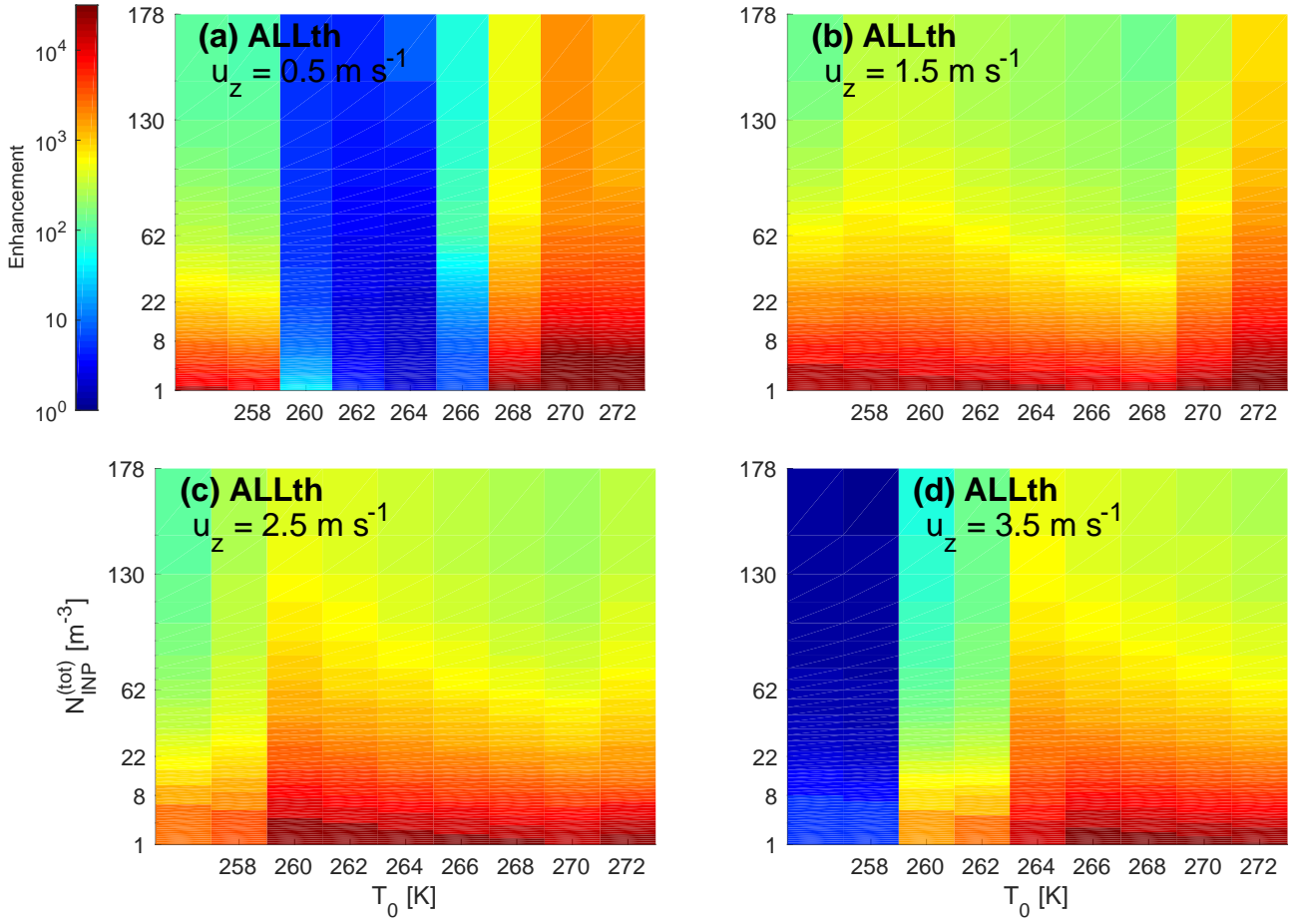


Figure S5. Ice crystal number concentration enhancement, i.e., $N_{ice}(t_{end})/N_{INP}(t_{end})$, for the thermodynamics simulations at various values of $N_{INP}^{(tot)}$, the total INP number in the parcel, and T_0 , the initial temperature. Red indicates a larger enhancement per INP. All panels show the enhancement when all secondary nucleation processes are active and with increasing updraft velocity u_z from panel (a) to (b) to (c) to (d).

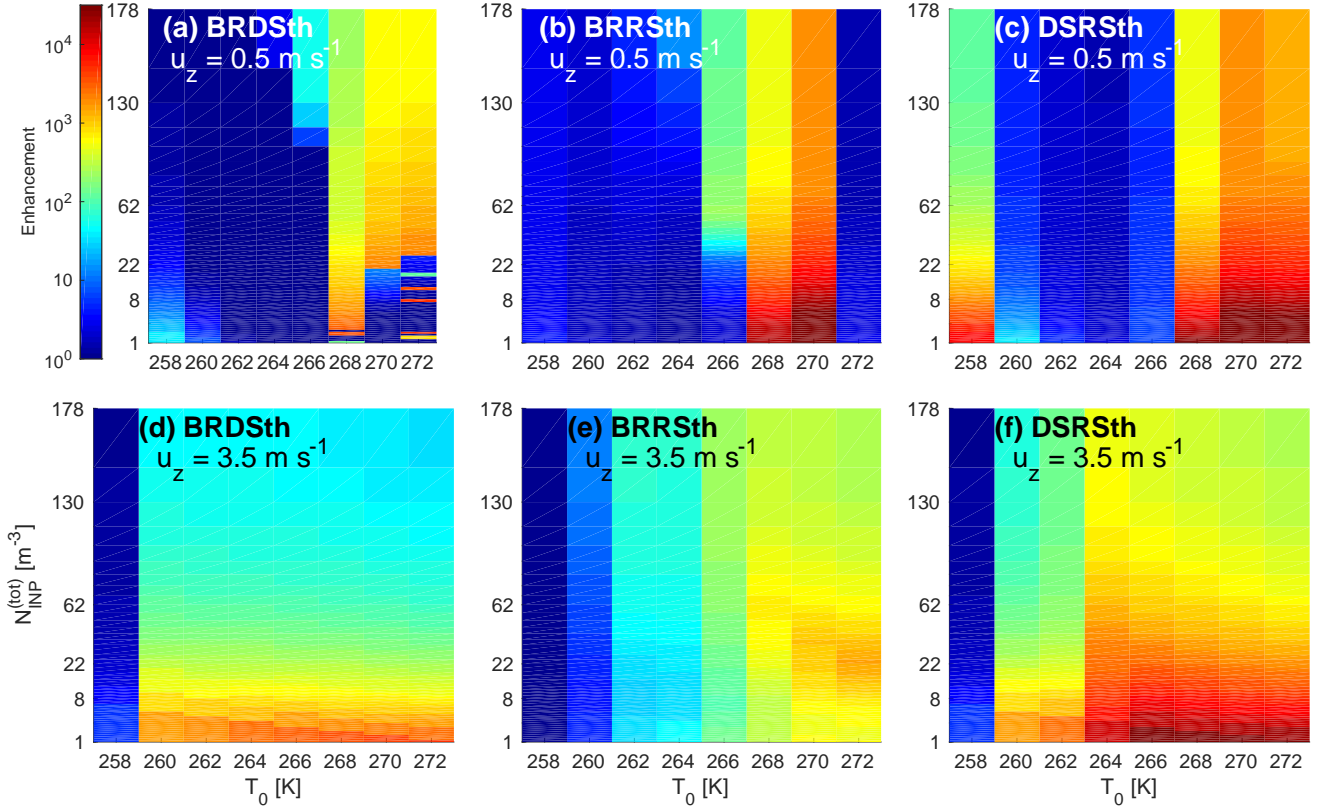


Figure S6. Ice crystal number concentration enhancement, i.e., $N_{ice}(t_{end})/N_{INP}(t_{end})$, for the thermodynamics simulations at various values of $N_{INP}^{(tot)}$, the total INP number in the parcel, and T_0 , the initial temperature. These are shown for various combinations of two secondary nucleation processes. Panels (a), (b), and (c) show the enhancements at a low, stratiform-like u_z of 0.5 m s^{-1} , and panels (d), (e), and (f) show them at higher, convective ones of 3.5 m s^{-1} .

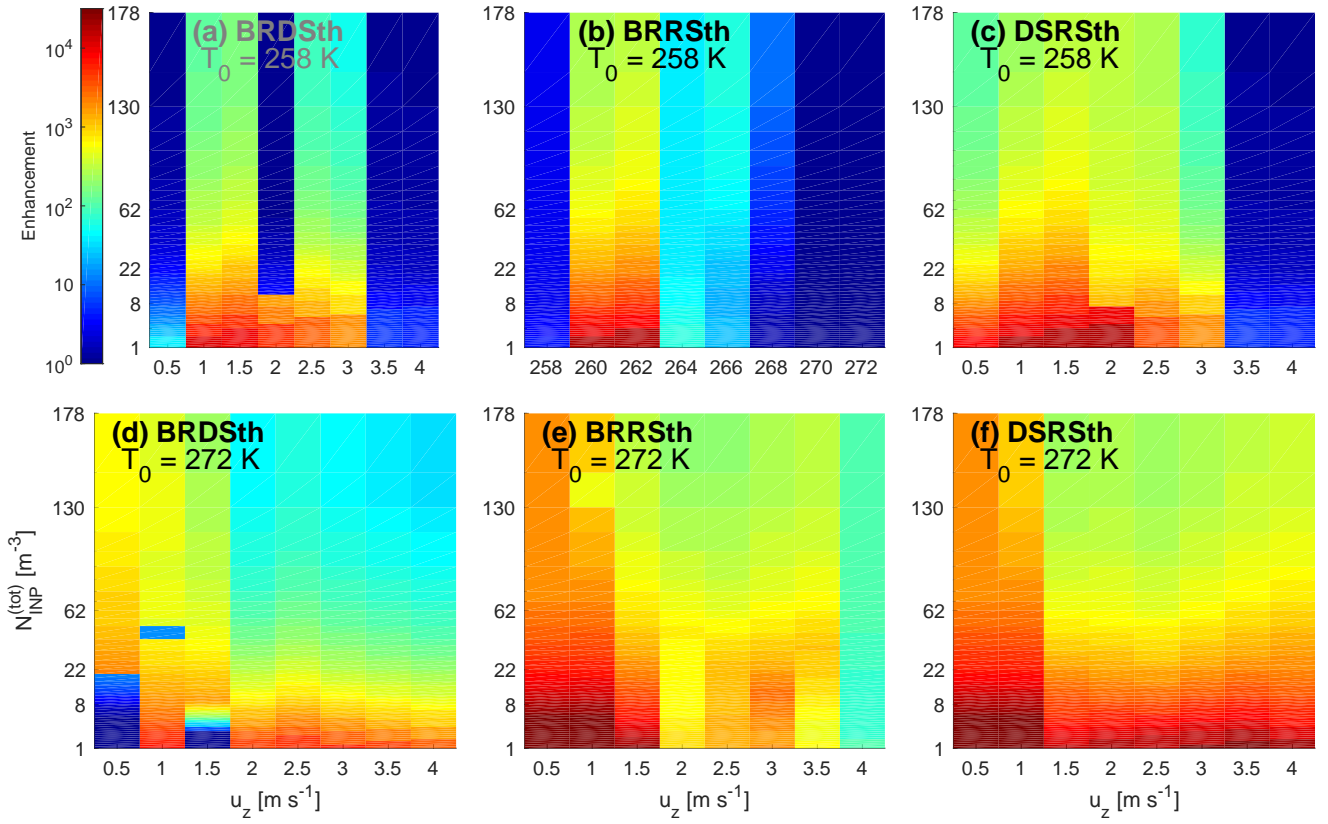


Figure S7. Ice crystal number concentration enhancement, i.e., $N_{ice}(t_{end})/N_{INP}(t_{end})$, for the thermodynamics simulations at various values of $N_{INP}^{(tot)}$, the total INP number in the parcel, and u_z , the updraft velocity. These are shown for various combinations of two secondary nucleation processes. Panels (a), (b), and (c) show the enhancements for a colder cloud base temperature of 258 K, and panels (d), (e), and (f) show them at a warmer one of 272 K.

Table S1. Default parameter values from simulations and their sources

Parameter	Value	Source
Fragment number		
$\aleph_{RS} = F_{RS} \rho_w \frac{\pi}{6} D_R^3$	$F_{RS} = 3 \times 10^8 \text{ frag (kg rime)}^{-1}$	Hallett and Mossop (1974)
$\aleph_{BR} = F_{BR}(T - T_{min})^{1.2} e^{-(T-T_{min})/5}$	$F_{BR} = 280$	Takahashi et al. (1995)
	$T_{min} = 252 \text{ K}$	
$\aleph_{DS} = F_{DS} D_R^4 p_{fr}(t, T, D) p_{sh}(T)$	$p_{sh} = 0.2\mathcal{N}(258 \text{ K}, 10 \text{ K})$	Droplet levitation experiments
	$p_{fr} = 1 - \exp[-\frac{\pi}{6} D^3 t K \exp(A(273 - T) - 1)]$	Bigg (1953)
$\aleph_{DS}^{(coll)} = F_{DS} D_R^4 p_{sh}(T)$	p_{sh} as above	Droplet levitation experiments
	$F_{DS} = 2.5 \times 10^{-11} \text{ frag (drop diam [\mu m])}^{-4}$	Lawson et al. (2015)
$\aleph_{DS}^{(sig)} = \frac{\alpha p_{fr}(t, T, D) p_{sh}(T)}{1 + \exp[-\beta(D - \gamma)]}$	$\alpha = 10; \beta = -0.016$ $\gamma = 500$	Droplet levitation experiments
Initial conditions		
N_{X0}	0 cm^{-3}	
$T_0, P_0, s_{w,0}$	$272 \text{ K}, 680 \text{ hPa}, 10^{-6}\%$	
r_{d0}, r_{r0}, r_{R0}	$1, 12, 25 \mu\text{m}$	Mossop (1978, 1985)
r_{i0}, a_{g0}, a_{G0}	$5, 50, 200 \mu\text{m}$	Zhang et al. (2014)
		Reinking (1975)
Time scales		
τ_d, τ_r, τ_R	$5, 15, 25 \text{ min}$	Approximate solution
τ_i, τ_g, τ_G	$7.5, 20, 17.5 \text{ min}$	of growth equations
Droplet spectrum		
k_{CCN}, N_{CCN}	$0.308, 100 \text{ cm}^{-3}$	(Hegg et al., 1992)
Updraft u_z	2 m s^{-1}	(Korolev and Field, 2007)
Time step Δt	3 sec	

References

- Bigg, E. K.: The formation of atmospheric ice crystals by the freezing of droplets, 79, 510–519, doi:10.1002/qj.49707934207, 1953.
- Hallett, J. and Mossop, S. C.: Production of secondary ice particles during the riming process, *Nature*, 249, 26–28, doi:10.1038/249026a0, 1974.
- 5 Hegg, D. A., Radke, L. F., and Hobbs, P. V.: Measurements of Aitken nuclei and cloud condensation nuclei in the marine atmosphere and their relation to the DMS-cloud-climate hypothesis, *J. Geophys. Res. - Atm.*, 97, 7659–7660, 1992.
- Korolev, A. and Field, P. R.: The effect of dynamics on mixed-phase clouds: Theoretical considerations, *J. Atmos. Sci.*, 65, 66–86, doi:10.1175/2007JAS2355.1, 2007.
- Lawson, R. P., Woods, S., and Morrison, H.: The microphysics of ice and precipitation development in tropical cumulus clouds, *J. Atmos. Sci.*,
10 72, 2429–2445, doi:10.1175/JAS-D-14-0274.1, 2015.
- Mossop, S. C.: The influence of drop size distribution on the production of secondary ice particles during graupel growth, *Q. J. R. Met. Soc.*, 104, 323–330, doi:10.1002/qj.49710444007, 1978.
- Mossop, S. C.: Secondary ice particle production during rime growth: The effect of drop size distribution and rimer velocity, *Q. J. R. Meteorol. Soc.*, 111, 1113–1124, doi:10.1002/qj.49711147012, 1985.
- 15 Reinking, R. F.: Formation of graupel, *J. Appl. Meteorol.*, 14, 745–754, doi:10.1175/1520-0450(1975)014, 1975.
- Takahashi, T., Nagao, Y., and Kushiyama, Y.: Possible high ice particle production during graupel-graupel collisions, *J. Atmos. Sci.*, 52, 4523–4527, doi:10.1175/1520-0469, 1995.
- Zhang, D., Wang, Z., Heymsfield, A., Fan, J., and Luo, T.: Ice concentration retrieval in stratiform mixed-phase clouds using cloud radar reflectivity measurements and 1D ice growth model simulations, *J. Atmos. Sci.*, 71, 3613–3635, doi:10.1175/JAS-D-13-0354.1, 2014.